

Effects of Various Baffle Designs on Acoustic Characteristics in Combustion Chamber of Liquid Rocket Engine

Chae Hoon Sohn*

Department of Aerospace Engineering, Chosun University, Gwangju 501-759, Korea

Seong-Ku Kim, Young-Mog Kim

Korea Aerospace Research Institute, POBox 113, Yusong, Daejeon 305-600, Korea

Effects of various baffle designs on acoustic characteristics in combustion chamber are numerically investigated by adopting linear acoustic analysis. A hub-blade configuration with five blades is selected as a candidate baffle and five variants of baffles with various specifications are designed depending on baffle height and hub position. As damping parameters, natural-frequency shift and damping factor are considered and the damping capacity of various baffle designs is evaluated. Increase in baffle height results in more damping capacity and the hub position affects appreciably the damping of the first radial resonant mode. Depending on baffle height, two close resonant modes could be overlapped and thereby the damping factor for one resonant mode is increased exceedingly. The present procedure based on acoustic analysis is expected to be a useful tool to predict acoustic field in combustion chamber and to design the passive control devices such as baffle and acoustic resonator.

Key Words : Baffle, Acoustic Characteristics, Damping Capacity, Resonant Modes, Combustion Chamber

1. Introduction

Combustion instability that results from sound-wave amplification is called acoustic instability, which has long gained significant interest in propulsion systems. Under acoustic instability, pressure oscillations are amplified through in-phase heat addition/extraction from combustion. It may lead to an intense pressure fluctuation as well as excessive heat transfer to combustor wall in combustion systems such as solid and liquid propellant rocket engines, ramjets, turbojet thrust augmentors, utility boilers, and furnaces (McManus et al., 1993). Accordingly, it has caused common problems in the course of engine development, i.e., thermal damage on in-

jector face plate and combustor wall, severe mechanical vibration of rocket body, and unpredictable malfunction of engines, etc. To understand this phenomenon, there have been conducted lots of fundamental works (Harrje and Reardon, 1972 ; Lee et al., 2003 ; Seo, 2003 ; Yang et al., 2003), but it is still being pursued.

There are two methods in the control of acoustic instability, classified into passive and active controls (Culick and Yang, 1995). Passive control is to attenuate acoustic wave using devices such as baffles, resonators, and acoustic liners. Although active control is studied and tested recently as an improved control method, the most reliable method to suppress acoustic-pressure oscillation is still to install baffle on the injector face plate as shown in Fig. 1.

In understanding of acoustic instability, combustion is of particular interest because it is the fundamental source of thermal energy that can be fed to amplify and sustain acoustic oscillations (Flefil et al., 1996 ; Sohn et al., 1996). But,

* Corresponding Author,

E-mail : chsohn@chosun.ac.kr

TEL : +82-62-230-7123; FAX : +82-62-230-7123

Department of Aerospace Engineering, Chosun University, Gwangju 501-759, Korea. (Manuscript Received February 5, 2003; Revised August 20, 2003)

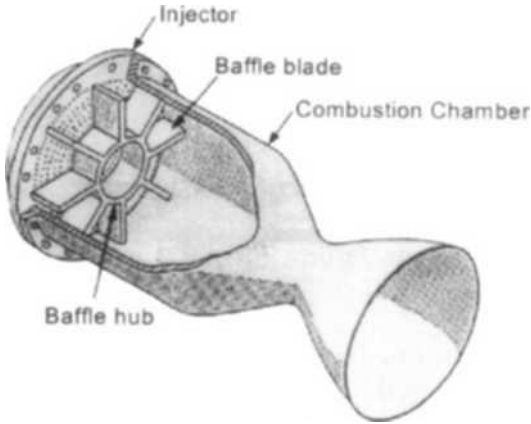


Fig. 1 Schematic diagram of baffled combustion chamber

reactive flow field established in liquid propellant rocket engine includes various elementary processes such as liquid injection, jet breakup, droplet formation, atomization, vaporization, fuel/oxidizer mixing, chemical reaction, and turbulence. It is rather complex to predict and not completely known yet. Accordingly, it is still formidable task to simulate acoustic amplification through interaction between acoustic wave and heat release rate. But, previous experimental works (Harrje and Reardon, 1972; NASA, 1974) showed that effects of baffle on acoustic damping investigated in cold flow corresponds to those in reactive flow field with negligible error. Based on this approximation, several acoustic tests and analyses were carried out successfully for practical baffle design (Harrje and Reardon, 1972; Sohn, 2002; Wicker et al., 1995; Yang et al., 1995) and especially, the acoustic effects of blade baffle and hub-blade baffle were extensively investigated through effective linear acoustic analysis in Sohn's work (2002). The acoustic damping mechanism of baffle is described elsewhere (Wicker et al., 1995; Yoon and Yoon, 1997) but not completely well-known yet.

In this study, baffle height and hub position are selected as design parameters of hub-blade baffle with five blades. Depending on the various combination of baffle height and hub position, five-variant baffles are employed and the damping effects of each variant on the major acoustic

modes are intensively investigated through the acoustic analysis adopted in the previous work (Sohn, 2002). It should be noted that only acoustic oscillation is investigated here without considering the coupling with heat release rate from the flame.

2. Numerical Methods and Models

2.1 Numerical methods

The acoustic field in combustion chamber is calculated through linear acoustic analysis and it is obtained by solving the following wave equation

$$\frac{1}{c^2} \frac{\partial^2 p}{\partial t^2} - \nabla^2 p = 0 \quad (1)$$

where p is the pressure fluctuation caused by acoustic-wave propagation, t is the time, c is the sound speed, and ∇^2 is the Laplacian operator. The derivation of Eq. (1), the introduced approximations, and its boundary conditions are described in detail in elsewhere (Zucrow and Hoffman, 1977).

The wave equation can be solved effectively by finite element method (FEM) and Galerkin method, which is one of FEMs, is used here (Chapra and Canale, 1989; SAS, 1993). Details on solution procedures and principles based on Galerkin method can be found in the literature (SAS, 1993). As a solver of the wave equation, ANSYS code is adopted in this study, which has been validated for acoustic analysis (Kang and Yoon, 1994; SAS, 1992).

2.2 Models

The selected combustion chamber and grid system are shown in Fig. 2, where the expansion nozzle part is omitted because it does not affect the acoustic field in the combustor part. The principal dimensions are the axial length, L , of 452 mm, the chamber diameter, D_{ch} , of 420 mm, and the nozzle throat diameter, D_{nt} , of 152.5 mm. As shown in this figure, the converging part of chamber has abrupt change of its cross-section due to relatively small throat diameter. In practical reactive flow of rocket engine, the sonic

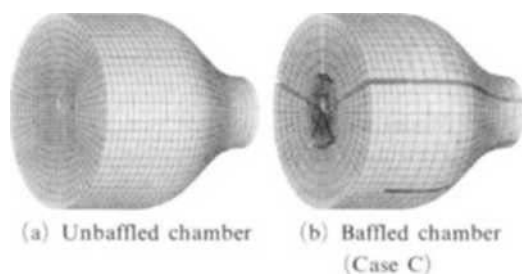


Fig. 2 Geometries and computational grids in unbauffed and bauffed chambers

condition is formed at the nozzle throat and thus, the throat can be considered to be acoustically closed end (Zucrow and Hoffman, 1977). Accordingly, wall boundary condition can be applied at the throat and all of outer boundaries surrounding fluid are regarded as wall. The fluid in the chamber is air of which density is 1.21 kg/m^3 and its sound speed is 340 m/s at 15.5°C . In analyzing the acoustic field in unbauffed chamber, i.e., chamber without baffle installation, about 23,000 elements are used for numerical calculation and in the other cases, the same order of the number of elements is adopted. This number of elements has been found to be enough to simulate acoustic behavior accurately in the present chamber.

As shown in Fig. 2(b), the typical hub-blade baffle with five blades is adopted here and the thickness of hub and blades is 10 mm in any case. As for hub diameter, D_H , and baffle height, i.e., baffle axial length, L_B , there are design criteria based on numerous engine tests (NASA, 1974; Shibanov, 2002). Although the criteria have not been supported by a firm theoretical verification, practical baffle designs have followed them. According to that criteria, the hub is typically located so that D_H/D_{ch} ranges from 0.3 to 0.4. And it is desirable to make L_B/D_{ch} be between 0.1 and 0.3. Considering these criteria, the baffle with $D_H=150 \text{ mm}$ and $L_B=85 \text{ mm}$ is selected as a baseline. With this baseline, several variants are designed and listed in Table 1, where $D_{H,i}$ and $D_{H,o}$ denote inner and outer diameters of the hub, respectively. As indicated in this table, Cases A to D are made to investigate the effects of baffle axial length on acoustic behavior

Table 1 Specifications of hub-blade baffles

CASE	L_B [mm]	$D_{H,i}$ [mm]	$D_{H,o}$ [mm]	Comment
A	65	140	160	$L_B \downarrow$
B	70	140	160	$L_B \downarrow$
C	85	140	160	Baseline
D	100	140	160	$L_B \uparrow$
E	85	260	280	$D_H \uparrow$

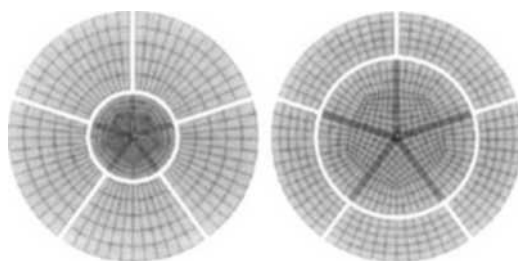


Fig. 3 Geometries and computational grids on cross-section near injector plate in bauffed chambers

and Cases C and E are for the effects of hub position. In the Case E with $D_H=270 \text{ mm}$, the hub is located at the node of acoustic-pressure oscillation, which corresponds to the anti-node of acoustic-velocity oscillation (Zucrow and Hoffman, 1977). Figure 3 shows the grid systems on the cross-section near injector plate in Cases A to D and E.

2.3 Numerical strategy

The acoustic effects of baffle are identified by two factors, i.e., the shift of natural or resonant frequency and the acoustic damping factor. To quantify them, modal and harmonic analyses are conducted, respectively (Sohn, 2002). In harmonic analysis, sound source is positioned on small area near the combustor wall, where sinusoidal sine wave with the specific frequency is generated numerically as a function of time, and the resultant pattern of acoustic oscillation is calculated. And thereby, natural acoustic modes, i.e., the first (1T), second (2T), and higher (3T, ...) tangential modes, radial modes (1R, 2R, ...),

longitudinal modes (1L, 2L, ...), and combined modes (1L1T, 1T1R, ...), are identified, and acoustic-pressure responses to acoustic excitation and the damping factors are calculated. The sweeping frequency of acoustic excitation from sound source with the amplitude of 10 Pa ranges from 400 to 1,000 Hz here. The monitoring point is near combustor wall at the opposite side to sound source on the identical cross-section, where the pressure amplitude is monitored.

The acoustic damping capacity of baffle is represented by damping factor, η , which is defined from bandwidth method (Laudien et al., 1995) as

$$\eta = \frac{f_2 - f_1}{f_{peak}} \quad (2)$$

where f_{peak} is the frequency at which the peak response (p_{peak}) is calculated, f_1 and f_2 are the frequencies at which the pressure amplitude corresponds to $p_{peak}/\sqrt{2}$ ($f_2 > f_1$). This equation indicates that the damping factor becomes higher as the bandwidth normalized by the peak frequency, f_{peak} , is broadened on the plane of the excitation frequency vs. acoustic-pressure response. In calculating the factor, boundary absorption coefficient, β , needs to be evaluated for harmonic analysis, which depends on the surface mechanical property of combustor wall and injector face plate. It is evaluated to be 0.005 from the experimental result (Ko et al., 2001). But, its absolute value is trivial in investigating the damping effect of baffle since the damping factor is linearly proportional to the value of β .

3. Results and Discussions

3.1 Modal analysis

The major natural frequencies in unbaffled and baffled chambers are calculated and summarized in Table 2. Baffle installation affects little the first longitudinal mode (1L) and 1L1T, but it decreases appreciably the natural frequencies of transverse modes. The frequencies of the two lowest modes, f_{1L} and f_{1T} , which are of particular interest in acoustic instability of liquid rocket engine, are calculated over the wide range of baffle axial length and shown in Fig. 4. The value of f_{1L} is maintained at a nearly constant value irrespective of baffle axial length, L_B , while the value of f_{1T} decreases with L_B . The crossover baffle length is about 60 mm. Comparing Case E ($L_B=85$ mm, $D_H=270$ mm) with Case C ($L_B=85$ mm, $D_H=150$ mm), the shift of f_{1T} is less than in Case C, but that of f_{1R} is more as shown in Table 2. Concerning 2T and 1R, natural frequencies decrease more with baffle length. These results imply that the longer baffle has more appreciable effect on acoustic damping and the hub with larger diameter of $D_H=270$ mm has less/more damping effect of the first tangential/radial mode. The former finding is in a good agreement with the experimental work (Harrje and Reardon, 1972).

3.2 Harmonic analysis

Acoustic responses to pressure oscillation with the excitation frequency of 400 to 550 Hz are

Table 2 Resonant frequencies of the major acoustic modes in unbaffled and baffled chambers

Mode	Unbaffled	Case A	Case B	Case C	Case D	Case E
1L	462.1	465.6	465.8	466.0	465.9	466.4
1T	500.3	458.2 (8.4% ↓)	451.9 (9.7% ↓)	431.7 (13.7% ↓)	410.2 (18.0% ↓)	454.2 (9.2% ↓)
1L1T	791.0	747.8 (5.5% ↓)	747.5 (5.5% ↓)	753.2 (4.8% ↓)	744.6 (5.9% ↓)	746.5 (5.6% ↓)
2T	811.3	696.7 (14.1% ↓)	677.7 (16.5% ↓)	620.6 (23.5% ↓)	567.4 (30.1% ↓)	633.0 (22.0% ↓)
1R	1018.7	765.6 (24.8% ↓)	762.3 (25.2% ↓)	700.2 (31.3% ↓)	629.5 (38.2% ↓)	665.9 (34.6% ↓)

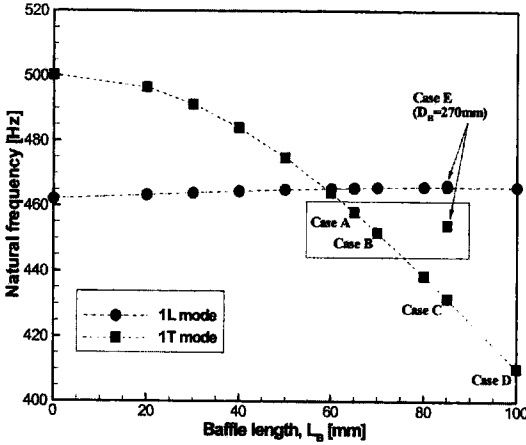


Fig. 4 Resonant frequencies of 1L and 1T modes as a function of baffle length

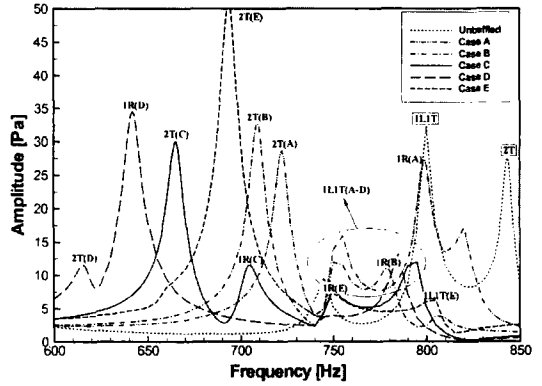


Fig. 6 Acoustic pressure responses of chamber to acoustic excitation in the frequency range of 1L1T, 2T, and 1R modes ($\Delta=5$ Hz)

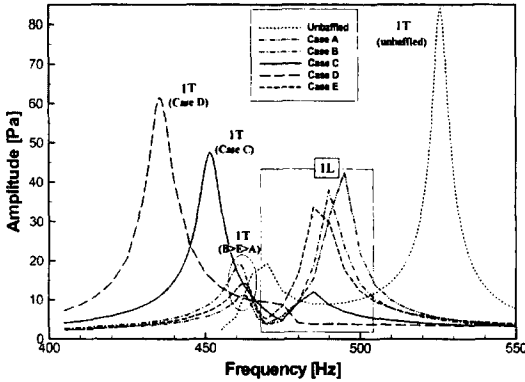


Fig. 5 Acoustic pressure responses of chamber to acoustic excitation in the frequency range of 1L and 1T modes ($\Delta=5$ Hz)

calculated and shown in Fig. 5. The increment of the frequency is 5 Hz. In unbuffered chamber, the amplitude of 1T is much higher than that of 1L and the absolute value of its amplitude is over 80 Pa, which is so high compared with the amplitude of the imposed pressure wave, 10 Pa. This indicates that the adopted chamber here are the most sensitive to acoustic oscillation of the first tangential mode. This figure shows that baffle installation causes the value of f_{1T} to decrease, which is already found through modal analysis in the preceding section. From the responses in Cases C and D, in which baffle is installed, the amplitude of 1T is still higher than that of 1L. But, in Cases A, B, and E, the amplitude of 1T is

rather lower than that of 1L. It is worthy of note that this results from the mode overlap or interference between 1T and 1L because f_{1T} and f_{1L} are much close to each other in Cases A, B, and E. As a result, the mode overlap causes one mode to be attenuated or amplified additionally.

Acoustic responses in high-frequency range are shown in Fig. 6, which shows the similar trend of 2T and 1R to that of 1T in that baffle length has significant effect on those acoustic modes. On the other hand, the mode of 1L1T is affected little by baffle length and hub diameter.

Based on the harmonic analyses, damping factors of the major acoustic modes are calculated from Eq. (2) and summarized in Table 3. In calculating damping factor, the increment of the frequency is 0.5 Hz, which has been verified to be small enough to produce accurate value of damping factor. Damping factor ratio is the normalized damping factor by the damping factor in unbuffered chamber. From this table, it is found that baffle installation increases the damping factor appreciably, which indicates the combustion stabilization effect of baffle. As predicted from the literature (Harrje and Reardon, 1972), the damping factor increases in proportion to baffle length. But, there are some exceptions, i.e., in 1T of Cases A and E, 2T of Case D, and 1R of Case D. The values of η_{1T} in Cases A and E with $L_B=65$ and 85 mm, respectively, are higher rather than that in Case D which has the longest baffle

Table 3 Damping factors of the major acoustic modes in unbaffled and baffled chambers

Mode		Unbaffled	Case A	Case B	Case C	Case D	Case E
1T	damping factor [%]	0.945	1.841	1.583	1.614	1.775	1.892
	ratio	1.000	1.948	1.675	1.708	1.878	2.002
2T	damping factor [%]	0.693	1.157	1.206	1.357	2.454	1.358
	ratio	1.000	1.670	1.740	1.958	3.541	1.960
1R	damping factor [%]	0.555	1.112		1.581	1.537	2.466
	ratio	1.000	2.004		2.849	2.769	4.443

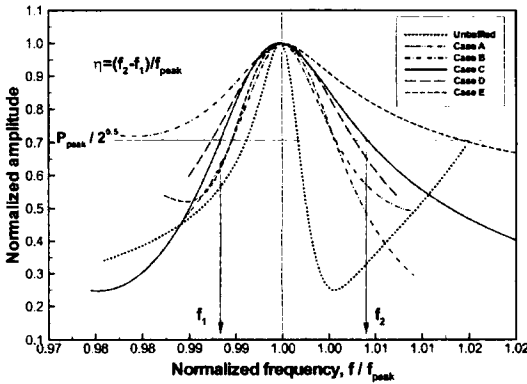


Fig. 7 Damping of the first radial modes in unbaffled and baffled chambers

of 100 mm. This is because 1T mode in two cases of A and E is overlapped with 1L mode and thereby acoustic oscillation of 1T mode is attenuated appreciably, leading to increase in η_{1T} . This reasoning is also supported by harmonic analysis shown in Fig. 5. The relatively higher (lower) value of η_{2T} (η_{1R}) in Case D, compared to the other cases, also results from the mode overlap or interference between 2T and 1R modes. Additionally, it is worthy of note that there cannot be calculated η_{1R} in Case B. This is illustrated in Fig. 7, where f_1 cannot be found based on Eq. (2). In this case, f_{1R} is much close to f_{1L1T} as shown in Fig. 6 and thus, 1R mode cancels out significantly, leading to ambiguous resonance at 1R mode. This acoustic attenuation/amplification of a specific mode due to the mode overlap is the additional effect of baffle installation, which is new finding, and it is worth while to investigate

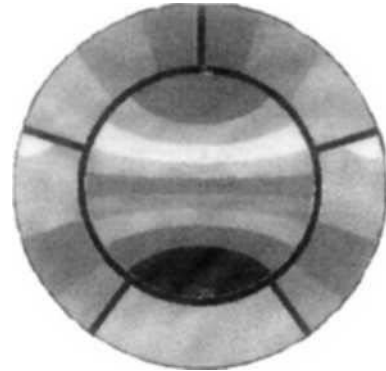


Fig. 8 Acoustic field resonated at the first sub-tangential mode in baffled chamber of Case E

this phenomenon in more detail as a future work.

In Case E ($D_H/D_{Ch}=0.642$), where the hub is positioned at the pressure node of 1R mode, the value of η_{1R} is much higher than in the other cases ($D_H/D_{Ch}=0.357$). This verifies the theoretical prediction from fundamentals of acoustics (Hartje and Reardon, 1972; Sohn, 2001). However, as aforementioned, the baffle of Case E is not recommended in that it has smaller shift of f_{1T} than in Case C. In addition, the present analysis shows that the chamber of Case E could be resonated at the sub-tangential mode in the field confined by the hub, which is illustrated in Fig. 8. In a similar form to the first ordinary tangential mode in the chamber, the first sub-tangential mode in the hub is evidently shown, which could trigger the tangential-mode instability.

4. Concluding Remarks

Acoustic behavior in combustion chamber of liquid rocket engine has been numerically investigated through linear acoustic analysis. Hub and five-blade baffles with various specifications are installed in the chamber, and the two design parameters are baffle axial length and hub position. Modal and harmonic analyses produce the resonant frequencies and acoustic-pressure responses in each specification of baffled chamber. Acoustic damping effect of baffle are judged by the shift of resonant frequencies and the damping factor for each resonant mode.

Baffle installation has appreciable effects on combustion stabilization and the effect is more appreciable as baffle length increases. Concerning damping of 1R mode only, it is the most effective to position the hub at the node of pressure oscillation. Depending on chamber geometry and baffle length, the mode overlap could show up when two modes are close to each other, and thereby, the additional acoustic attenuation/amplification at a specific mode results. Thus, the phenomenon of the mode overlap should be considered in designing baffle. The acoustic prediction conducted in this study is helpful to understand acoustic behavior in baffled chamber and to design the effective baffle which suppresses acoustic instability.

Acknowledgment

This study was supported in part by research funds from Chosun University, 2002.

References

- Chapra, S. C. and Canale, R. P., 1989, *Numerical Methods for Engineers*, 2nd ed., McGraw-Hill, Singapore.
- Culick, F. E. C. and Yang, V., 1995, in *Liquid Rocket Engine Combustion Instability* (V. Yang, and W. E. Anderson, eds.), *Progress in Astronautics and Aeronautics*, Vol. 169, AIAA, Washington DC, pp. 3~38.
- Fleifil, M., Annaswamy, A. M., Ghoniem, Z. A. and Ghoniem, A. F., 1996, "Response of a Laminar Premixed Flame to Flow Oscillations: A Kinematic Model and Thermoacoustic Instability Results," *Combustion and Flame*, Vol. 106, pp. 487~510.
- Harrje, D. J. and Reardon, F. H. (eds.), 1972, *Liquid Propellant Rocket Combustion Instability*, NASA SP-194.
- Kang, K. T. and Yoon, J. K., 1994, "Analysis of Combustion Instability in a Smokeless Propellant Rocket Motor," *Transactions of The KSME (B)*, Vol. 18, No. 11, pp. 3032~3038.
- Ko, Y. S., Lee, K. J., Kang, D. H. and Kim, H. M., 2001, KARI (Korea Aerospace Research Institute) Test Note PPTD-01-13.
- Laudien, E., Pongratz, R., Pierro, R. and Preklik, D., 1995, in *Liquid Rocket Engine Combustion Instability* (V. Yang, and W. E. Anderson, eds.), *Progress in Astronautics and Aeronautics*, Vol. 169, AIAA, Washington DC, pp. 377~399.
- Lee, C., Lee, J. W. and Byun, D. Y., 2003, "Transient Analysis of Hybrid Rocket Combustion by the Zeldovich-Novozhilov Method," *KSME International Journal*, Vol. 17, No. 10, pp. 1572~1582.
- McManus, K. R., Poinso, T. and Candel, S. M., 1993, "A Review of Active Control of Combustion Instabilities," *Progress in Energy and Combustion Science*, Vol. 19, pp. 1~29.
- NASA, 1974, "Liquid Rocket Engine Combustion Stabilization Devices," NASA SP-8113.
- SAS, 1992, *ANSYS User's Manual for revision 5.0*, Volume I, Procedures, Swanson Analysis Systems, Inc., Houston, PA.
- SAS, 1993, *ANSYS User's Manual for revision 5.0*, Volume IV, Theory, Swanson Analysis Systems, Inc., Houston, PA.
- Seo, S., 2003, "Combustion Instability Mechanism of a Lean Premixed Gas Turbine Combustor," *KSME International Journal*, Vol. 17, No. 6, pp. 906~913.
- Shibanov, A. A., 2002, Personal Communications.
- Sohn, C. H., 2001, "Effect of Injector Array on Acoustic Instability in Liquid Rocket Engines," *Journal of The Korean Society for Aeronautical*

and Space Sciences, Vol. 29, No. 6, pp. 76~83.

Sohn, C. H., 2002, "A Numerical Study on Acoustic Behavior in Baffled Combustion Chambers," *Transactions of the KSME(B)*, Vol. 27, No. 1, pp. 966~975.

Sohn, C. H., Chung, S. H., Kim, J. S. and Williams, F. A., 1996, "Acoustic Response of Droplet Flames to Pressure Oscillations," *AIAA Journal*, Vol. 34, No. 9, pp. 1847~1854.

Wicker, J. M., Yoon, M. W. and Yang, V., 1995, "Linear and Non-linear Pressure Oscillations in Baffled Combustion Chambers," *Journal of Sound and Vibration*, Vol. 184, pp. 141~171.

Yang, V., Wicker, J. M. and Yoon, M. W., 1995, in *Liquid Rocket Engine Combustion Insta-*

bility (V. Yang, and W. E. Anderson, eds.), *Progress in Astronautics and Aeronautics*, Vol. 169, AIAA, Washington DC, pp. 357~376.

Yang, Y. J., Akamatsu, F. and Katsuki, M., 2003, "Characteristics of Self-excited Combustion Oscillation and Combustion Control by Forced Pulsating Mixture Supply," *KSME International Journal*, Vol. 17, No. 11, pp. 1820~1831.

Yoon, M. W. and Yoon, J. K., 1997, "Combustion Instability in Liquid Rocket Engines," *Journal of The Korean Society for Aeronautical and Space Sciences*, Vol. 25, No. 5, pp. 183~189.

Zucrow, M. J. and Hoffman, J. D., 1977, *Gas Dynamics*, Vol. II, John Wiley & Sons, Inc., New York.